

- ¹⁶Leeds and Northrup, student potentiometer.
- ¹⁷A. A. R. El Agib, *J. Sci. Instr.* **41**, 592 (1964).
- ¹⁸P. G. Klemens, in *Encyclopedia of Physics*, edited by S. Flügge (Springer-Verlag, Berlin, 1956), Vol. 14.
- ¹⁹R. H. Bogaard and A. N. Gerritsen, in *Thermal Conductivity*, edited by C. Y. Ho and R. E. Taylor (Plenum, New York, 1969), p. 185. The results presented in Figs. 2-4 contain those reported in this preliminary paper as well as the results of extended measurements to below 3 K with sample Cd C3 and a few alloys.
- ²⁰B. N. Aleksandrov, *Zh. Eksperim. i Teor. Fiz.* **43**, 399 (1962) [*Soviet Phys. JETP* **16**, 286 (1963)].
- ²¹P. Wyder, *Physik Kondensierten Materie* **3**, 263 (1965).
- ²²N. E. Phillips, *Phys. Rev.* **134**, 385 (1964).
- ²³P. L. Smith and N. M. Wolcott, *Phil. Mag.* **1**, 854 (1956).
- ²⁴R. S. Craig, C. A. Krier, L. W. Coffey, E. A. Bates, and W. E. Wallace, *J. Am. Chem. Soc.* **76**, 238 (1954).
- ²⁵C. W. Garland and J. Silverman, *Phys. Rev.* **119**, 1218 (1960).
- ²⁶M. Kohler, *Z. Physik* **126**, 495 (1949).
- ²⁷R. L. Powell, W. J. Hall, and H. M. Roder, *J. Appl. Phys.* **31**, 496 (1960).
- ²⁸For these and further considerations, see J. M. Ziman, *Electrons and Phonons* (Clarendon, Oxford, England, 1960), Chap. IX.
- ²⁹R. C. Jones, R. G. Goodrich, and L. M. Falicov, *Phys. Rev.* **174**, 672 (1968).
- ³⁰J. M. Ziman, *Phys. Rev.* **121**, 1320 (1961).
- ³¹R. L. Powell and W. A. Blanpied, *Natl. Bur. Std. (U.S.), Circ.* **556** (1954).
- ³²R. Berman and D. K. C. MacDonald, *Proc. Roy. Soc. (London)* **A209**, 368 (1951).
- ³³J. D. Filby and D. L. Martin, *Proc. Roy. Soc. (London)* **A276**, 187 (1963).
- ³⁴R. Berman and D. K. C. MacDonald, *Proc. Roy. Soc. (London)* **A211**, 122 (1952).
- ³⁵D. L. Martin, *Phys. Rev.* **141**, 576 (1966).
- ³⁶G. K. White, *Proc. Phys. Soc. (London)* **66A**, 844 (1953).
- ³⁷F. A. Andrews, R. T. Webber, and D. A. Spohr, *Phys. Rev.* **84**, 994 (1951).
- ³⁸W. T. Berg, *Phys. Rev.* **167**, 583 (1968).
- ³⁹R. E. Jones and A. M. Toxen, *Phys. Rev.* **120**, 1167 (1960).
- ⁴⁰C. A. Bryant and P. H. Keesom, *Phys. Rev.* **123**, 491 (1961).
- ⁴¹R. T. Webber and D. H. Spohr, *Phys. Rev.* **106**, 927 (1957).
- ⁴²B. Van der Hoeven and P. H. Keesom, *Phys. Rev.* **135**, 631 (1964).
- ⁴³J. A. Rayne, *J. Phys. Chem. Solids* **7**, 268 (1958).
- ⁴⁴J. M. Dishman and J. A. Rayne, *Phys. Rev.* **166**, 728 (1968).

Calorimetric Determination of the Density of Electronic States in α -Phase Indium Alloys. I. Alloys with Tin[†]

Marcel H. Lambert,* J. C. F. Brock,† and Norman E. Phillips
*Inorganic Materials Research Division of the Lawrence Radiation Laboratory and
 Department of Chemistry, University of California, Berkeley, California 94720*
 (Received 11 September 1970)

The low-temperature heat capacity of each of a series of indium-tin alloys containing 0-13 at. % tin has been measured, and the density of electronic states $N(E_F)$ and the Debye temperature Θ_0 evaluated. The electron-phonon coupling constant λ was calculated from the superconducting critical temperature T_c and Θ_0 , and was used to derive the band-structure density of states $N_{bs}(E_F)$. Both $N_{bs}(E_F)$ and λ increase more rapidly with increasing tin content above 9 at. % tin than below 9 at. %. These results are interpreted in terms of the Brillouin-zone-boundary-Fermi-surface interaction that has been postulated to explain the behavior of the lattice parameters and T_c . Comparison with band-structure calculations and experimental Fermi-surface studies for pure indium suggest that new parts of the Fermi surface appear in the third zone at this electron concentration.

I. INTRODUCTION

In recent years, a variety of elegant techniques for determining the geometry of the Fermi surface have been applied to pure metals, and the shape of the Fermi surface is now known in considerable detail for many of them. The addition of an alloying metal changes the Fermi surface by changing the conduction-electron/atom ratio Z , and also through

the effect of the different ion-core potential on the energy-momentum relation of the conduction electrons. Unfortunately, the techniques that have made the most important contributions to the determination of the Fermi-surface geometry of pure metals require long electron mean free paths and are therefore not applicable to alloys. As a consequence, very little is known about the changes in the Fermi surface that accompany alloying. Of the

various sources of information on the electronic structure of alloys, the low-temperature heat capacity is among the simplest to interpret because it gives unambiguously $N(E_F)$, the density of electronic states at the Fermi energy E_F . In practice, however, this does not contribute much to a knowledge of the Fermi surface unless considerable supplementary information is available. The α -phase alloys of indium seemed to provide an example of a system in which enough other information is available that a knowledge of the changes in $N(E_F)$ brought about by alloying might make a substantial contribution to an understanding of the accompanying changes in the Fermi surface.

The Fermi surface of pure indium has been determined relatively completely by direct experiments¹⁻⁶ and the band structure has also been studied theoretically.⁷⁻⁹ The electronic structure is similar to that predicted by the nearly free-electron model: a filled or nearly filled first zone, an extensive second-zone hole surface, and tubes of electrons along edges of the third zone. There are, however, some remaining uncertainties about the occupancy of some corners and edges in the second and third zones.

Indium has tetragonal symmetry and the face-centered tetragonal (fct) unit cell has an axial ratio $c/a \approx 1.08$. When Z is decreased by alloying with cadmium^{10,11} or mercury,¹² or increased by alloying with tin¹³ or lead,^{11,12} the fct phase with $c/a \geq 1$ remains stable in the region $2.95 \lesssim Z \lesssim 3.15$. Below $Z \approx 2.95$, a cubic phase is stable, and above $Z \approx 3.15$, the stable phase is an fct phase with $c/a < 1$. Throughout most of the region of stability of the α -phase alloys the available data show a smooth variation of the lattice parameters with Z . The c/a ratio increases, but at a decreasing rate with increasing Z . Near $Z = 2.98$ and 3.08 , however, precise measurements on alloys with closely spaced values of Z have shown a more complicated behavior. Merriam has reported "wiggles" in plots of the a and c dimensions vs Z near $Z = 3.08$ for both indium-tin¹⁴ and indium-lead,¹⁵ and near $Z = 2.98$ for indium-cadmium.¹⁶ The wiggles were not confirmed in lattice-parameter measurements on indium-cadmium by Ridley¹⁷ or in low-temperature lattice-parameter measurements on indium-lead by Preece and King.¹⁸ However, all the data are consistent with rapid changes in the slope of c/a vs Z near $Z = 2.98$ and 3.08 . The measurements by Ridley and by Preece and King show that the atomic volume varies linearly with Z throughout the regions $2.965 < Z < 3.00$ and $3.00 < Z < 3.11$, respectively. Changing the axial ratio of a metal at constant atomic volume changes the conduction-electron energy by changing the energy-momentum relations.¹⁹ The effect is greatest when the Fermi surface is close to contact with Brillouin-zone faces and is then

sensitive to their relative position, which is determined in part by the number of conduction electrons. These Brillouin-zone-boundary-Fermi-surface interactions can therefore affect the relative stability of the cubic and tetragonal phases, and contribute to the trend in the axial ratio with changing Z .^{19,20} The stability of the α -phase indium alloys has been discussed from this point of view by Yonamitsu.²¹ Interpretations of the trend in their c/a ratios with increasing Z based on a "pinning" of the Fermi surface at certain zone corners followed by breakthrough into a higher zone have also been developed.^{18,22}

Merriam and Von Herzen²³ discovered a change in the slope of T_c vs Z for indium-tin near $Z = 3.085$, and Merriam found similar effects in indium-lead^{14,15} near $Z = 3.075$, and in indium-cadmium^{16,24} near $Z = 2.98$. It was suggested^{14-16,23,24} that these effects had their origin in the same Brillouin-zone-boundary-Fermi-surface interactions that had been discussed in connection with the axial ratios. Havinga²⁵ has drawn attention to the fact that the variation of T_c with Z is approximately parabolic throughout the region $2.95 < Z < 3.15$ for the indium-cadmium and indium-tin alloys. For this reason he has questioned the reality of the Brillouin-zone-boundary effects near $Z = 2.98$ and 3.08 . It is certainly true that the two straight lines used to represent the T_c data in the regions $2.98 < Z < 3.00$ (indium-cadmium^{24,25}) and $3.00 < Z < 3.08$ (indium-tin^{15,23}) have different slopes and do not adequately represent the data near $Z = 0$. In view of the exponential dependence of T_c on parameters related to the electronic structure, it would be surprising indeed if the variation of T_c were linear throughout a range of Z in which T_c changes from 3.3 to 5.5 K and which is bounded by two qualitative changes in the Fermi surface. The significance of the straight lines is that they emphasize values of Z near which the derivative of T_c with respect to Z changes more rapidly than elsewhere. However, the breadth of the transition limits the precision of the T_c measurements and leaves a question as to whether there are discontinuities in the derivative, or merely sharp peaks in the second derivative. The shape of the T_c -vs- Z curve for indium-lead has been confirmed by Preece and King.¹⁸

Thus, there is good reason to expect abrupt changes in the Fermi surface of the α -phase indium alloys at predictable values of Z , and there is enough information on the Fermi surface of pure indium to hope that changes in $N(E_F)$ with Z could be interpreted in terms of changes in the Fermi surface. The occurrence of superconductivity in these alloys provides added incentive for heat-capacity measurements because the electron-phonon matrix elements that are related to T_c are the

same ones that determine the phonon enhancement of $N(E_F)$. The electron-phonon coupling constant λ can be estimated from T_c and the calorimetric data, and then used to calculate the phonon enhancement.²⁶ This permits a more rigorous comparison of the experimental $N(E_F)$ with band-structure calculations, which do not include phonon enhancement, than would otherwise be possible. Furthermore, comparisons of λ with $N(E_F)$ and with the Debye characteristic temperature Θ_0 would themselves be of interest. The indium-cadmium and indium-tin systems were chosen for the measurements because the effect of the substitutions on the lattice potential should be a minimum. In this paper, heat-capacity measurements on indium-tin alloys are reported. In a later paper,²⁷ similar measurements on indium-cadmium alloys will be presented.

II. EXPERIMENTAL PROCEDURE

The samples, each of which contained approximately 1 mole of alloy, were prepared by melting together weighed amounts of Cominco 99.9999% tin and indium under an inert atmosphere and stirring vigorously. The reported compositions are based on the weights of the components. All samples were annealed for approximately 200 h at 140°C immediately before the heat-capacity measurements. The 12.8% sample was cooled to liquid-N₂ temperature within 2 h of annealing to ensure retention of the α phase.

The same sample holder and calibrated germanium thermometer were used in all measurements. The thermometer had been calibrated against He⁴ vapor pressure and the susceptibility of a spherical crystal of cerium magnesium nitrate. The sample holder consisted of a stiff vertical copper stalk with a copper clamp for attachment to the sample at the lower end. The thermometer was mounted near the upper end of the stalk, 20 cm above the top of the sample, and the heater was placed near the sample. This arrangement was designed to permit the application of magnetic fields to the sample without affecting the thermometer calibration. Tests showed that fields of 1500 Oe at the sample had no measurable effect on the thermometer calibration, with the solenoid geometry used for the heat-capacity measurements. The relaxation time for thermal equilibrium in the complete assembly was too short to be observed (<1 sec), in agreement with estimates based on the heat capacity and thermal conductivity of copper, and on experience with similar copper-sample and copper-thermometer thermal contacts. The term proportional to T in the heat capacity of the sample holder was 18–26% of those in the samples; the T^3 term in the sample-holder heat capacity was a much smaller fraction of those in the samples. The heat capacity

of the empty sample holder was measured in separate experiments.

Two methods of cooling the samples were used. In the earlier measurements, the sample was cooled to 1 K in zero magnetic field using a mechanical heat switch; the heat switch was opened and further cooling obtained by adiabatic magnetization to a field of 1000–1500 Oe. This method usually gave starting temperatures of about 0.6 K for the heat-capacity measurements. The later measurements were made using He³ and a mechanical heat switch to cool to about 0.3 K, and the heat-capacity measurements were made in a field of 1000 Oe. For several samples measured by both techniques, the data agreed within the precision of the measurements.

The superconducting transitions were observed calorimetrically for most samples, partly as a check on homogeneity. For these measurements the stray magnetic field on the samples was adjusted to be less than 0.1 Oe.

III. RESULTS

The breadth and temperatures of the superconducting transitions observed calorimetrically are in good agreement with those reported by Merriam and Von Herzen.²³ In general, the breadth of the transition increased with increasing tin concentration. Furthermore, even for a sharp transition the discontinuity in heat capacity would decrease relative to the total heat capacity with increasing T_c , and therefore with increasing tin concentration. For these reasons the temperature range of the transition is less well defined for the higher concentrations. A typical transition for an intermediate concentration is shown in Fig. 1. In Fig. 2, the T_c values, with error bars indicating the breadth of the transitions, are compared with the values obtained by Merriam and Von Herzen.²³

Analysis of the data to separate γT , the electronic contribution to the normal-state heat capacity, is complicated by the presence of a hyperfine heat capacity, which is proportional to T^{-2} , and by the low value of Θ_0 . Since $\Theta_0 = 111$ K, the lattice heat

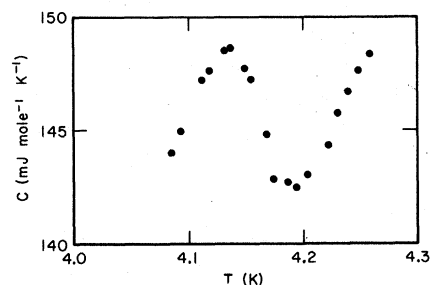


FIG. 1. Heat capacity of a 7.58 at. % tin in indium alloy near the superconducting critical temperature.

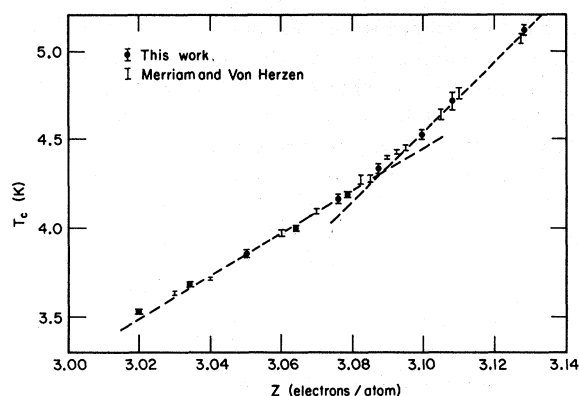


FIG. 2. Comparison of superconducting critical temperatures observed in this work with those reported in Ref. 23. The dashed lines are intended to emphasize the change in slope near $Z = 3.09$.

capacity is relatively large, and in fact comparable to the electronic heat capacity at 1 K. Furthermore, the lattice heat capacity deviates significantly²⁸ from T^3 at 2 K, and the measurements were therefore not extended above this temperature. Measurements below 0.5 K would include substantial hyperfine contributions and would not lead to much improvement in the precision of the γ values. Most of our data is at $T > 0.7$ K, and comparison with the known hyperfine heat capacity of pure indium²⁸ suggests that the hyperfine contribution is negligible at these temperatures. Consequently, we write the heat capacity as

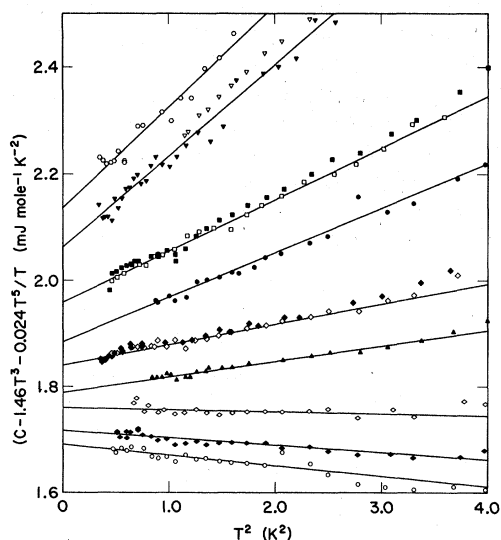


FIG. 3. Some typical heat-capacity data. From bottom to top, the data shown are for the 3.41, 5.03, 6.39, 7.84, 8.74, 9.94, 10.80, 11.91, and 12.83 at. % tin samples. Where open and closed symbols are used for the same sample, they distinguish between runs made by the two procedures described in the text.

$$C = \gamma T + \alpha T^3 + \beta T^5, \quad (1)$$

where we have retained the first two terms in the low-temperature approximation for the lattice heat capacity, and $\alpha = \frac{12}{5} \pi^4 R \Theta_0^{-3}$.

Two sets of values of γ and α were derived. The first set was obtained by inspection of plots of $(C - 1.46T^3 - 0.024T^5)/T$ vs T^2 and estimation of the limiting low-temperature slope. Some typical plots are shown in Fig. 3. The T^5 term subtracted for these plots was chosen because a preliminary inspection of the data showed that it would substantially reduce the curvature for all samples. A second set of values for γ and α and values of β were obtained by plotting $(C - \gamma'T)/T^3$ vs T^2 using a series of γ' values. Values of γ , α , and β were then assigned by picking the γ' value that gave the best straight line over the whole temperature range. The first method gave lower γ values and higher α values by amounts ranging between 0 and 0.5% for both parameters. In Table I, which gives the heat-capacity parameters for all samples, the values of γ and α are averages of those obtained by the two methods.

Table II compares the values of the coefficients in Eq. (1) for pure indium with those found in other experiments. The calorimetric measurements by Clement and Quinnell²⁹ did not extend below 1.7 K and were referred to an older temperature scale. The other five heat-capacity measurements are in much better agreement on the total heat capacity than on values of the individual parameters; the maximum discrepancy in total heat capacity at 1 K is 1%, but the maximum discrepancies in γ and α are, respectively, 5 and 12%. This is undoubtedly a consequence of the sensitivity of the values of γ and α to small errors in thermometer calibration and to the method of analyzing the data.

It is difficult to assign firm limits for the errors in our γ and α values. We have made no measure-

TABLE I. Heat-capacity parameters for indium-tin alloys.

at. % tin	γ ($\frac{\text{mJ}}{\text{mole K}^2}$)	α ($\frac{\text{mJ}}{\text{mole K}^4}$)	β ($\frac{\text{mJ}}{\text{mole K}^6}$)	T_c (K)
0	1.633	1.455	0.025	...
1.98	1.661	1.422	0.023	3.53
3.41	1.691	1.440	0.023	3.68
5.03	1.718	1.446	0.024	3.85 _s
6.39	1.761	1.456	0.025	4.00
7.58	1.782	1.486	0.024	4.16 _s
7.84	1.790	1.489	0.024	4.19
8.74	1.841	1.498	0.025	4.33 _s
9.94	1.890	1.546	0.021	4.53
10.80	1.958	1.557	0.026	4.71 _s
11.91	2.063	1.631	0.022	...
12.83	2.136	1.649	0.027	5.12

TABLE II. Heat-capacity parameters for indium.

Measurement	γ $\left(\frac{\text{mJ}}{\text{mole K}^2}\right)$	α $\left(\frac{\text{mJ}}{\text{mole K}^4}\right)$	β $\left(\frac{\text{mJ}}{\text{mole K}^6}\right)$
Heat capacity			
Clement and Quinell ^a	1.81	1.50	
Bryant and Keesom ^b	1.61	1.50	0.008
Bryant and Keesom	1.59	1.54	0.008
White and McCollum ^c	1.66	1.37	0.065
O'Neal and Phillips ^d	1.69	1.42	0.023
This work	1.63	1.46	0.025
Elastic constants			
Chandrasekhar and Rayne ^e		1.41	
Critical field			
Finnemore and Mapother ^f	1.66		

^aSee Ref. 29.^bSee Ref. 30.^cSee Ref. 31.^dSee Ref. 28.^eSee Ref. 32.^fSee Ref. 33.

ments with the same thermometer on a "standard" substance such as copper which could be compared with accepted values. However, the important source of systematic errors is the thermometer calibration (the energy measurements are accurate to a few hundredths of a percent) and this calibration was carried out by well-tested methods. Our past experience with these techniques suggests an accuracy of $\pm 0.5\%$, and this is consistent with the comparison with other recent data for indium in Table II. (We have also measured the heat capacities of tin and lead with the same sample holder and thermometer and obtained heat capacities, and values of γ and α , in good agreement with measurements that were based on independent thermometer calibrations.) The uncertainty in the γ and α values is greater than that in the heat capacity because the temperature dependence of the error in the temperature can introduce a spurious temperature dependence in the heat capacities, and the derived parameters for indium are particularly sensitive to such effects. Inspection of various plots of the data - for example, those shown in Fig. 3 - and the estimated $\pm 0.5\%$ maximum error in heat capacity suggest that γ and α are accurate to about 2%. For our present purposes it is the relative values of γ and α for different alloys that are of most interest. Since the thermometer calibration and procedure for data analysis was identi-

cal for all samples, we expect the precision of our parameters to be appreciably better than their accuracy. This expectation is borne out by inspection of plots of γ and α vs composition, which suggest a precision of approximately 0.5%.

The heat capacities of four indium-tin alloys between 0.8 and 9.7 at. % tin have also been measured by White and McCollum.³¹ The differences between their values for γ and α and ours are similar to the corresponding differences for pure indium (see Table II) except for their 4.9 at. % sample for which they report a relatively high γ value and a correspondingly low α value. Since only one sample is involved, we do not regard this as a serious disagreement with the trends for γ and α reported in Table I.

IV. DISCUSSION

A. Band Structure

Figures 4 and 5 show the dependence of Θ_0 and γ on composition. The smooth curve through the Θ_0 data (see Table III) shows no conspicuous changes of slope, and, in fact, the second derivative is constant to within a factor of 2 for $Z > 3.03$ and to within a factor of 2.5 over the whole range. In contrast, a smooth curve drawn as a "best fit" to the γ data would have a sharply peaked second derivative near 9 at. % tin. This difference in behavior is consistent with an abrupt change in electronic structure, e.g., the appearance of a new piece of the Fermi surface, since Θ_0 should be much less sensitive than γ to such a change. We interpret the Z dependence of γ as further support for the interpretations of the T_c and lattice-parameter data in terms of a Brillouin-zone-boundary-Fermi-surface interaction. The dashed lines in Fig. 5, which intersect at $Z = 3.09$, are good approximations to the Z dependence of γ for $3.02 < Z < 3.13$ except for the one point nearest $Z = 3.09$. That point suggests that there is no discontinuity in the derivative of γ with respect to Z . The pre-

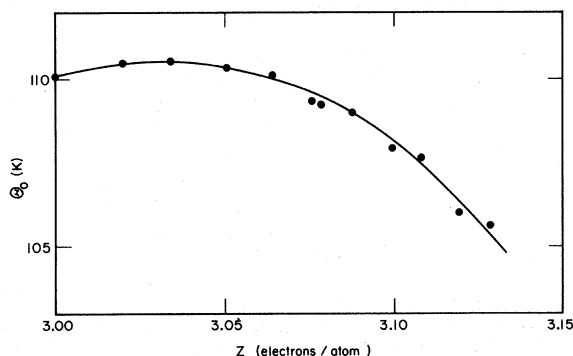


FIG. 4. Debye characteristic temperature as a function of the conduction-electron/atom ratio.

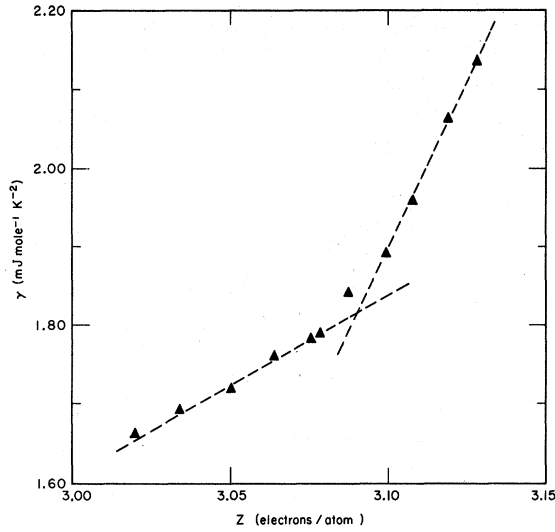


FIG. 5. Coefficient of the electronic heat capacity as a function of the conduction-electron/atom ratio. The dashed lines are intended to emphasize the change of slope near $Z = 3.09$.

cision of the γ values is not high enough for a single point to establish this conclusion with certainty, but the behavior of γ in this region is very similar to that of T_c , for which there are more data. It therefore seems probable that no discontinuity in slope actually occurs (unless there are several small unresolved discontinuities). It is possible that a discontinuity would have been observed in an ordered crystal, but it is smoothed out by the disorder or possible inhomogeneity in our samples. Shaw and Smith⁹ have shown that nonlocal effects lead to a considerable smoothing out of the structure in the density of states in liquid metals, and

TABLE III. Derived parameters for indium-tin alloys.

Z (electrons/atom)	T_c^a (K)	Θ_0 (K)	λ	$N_{bs}(E_F)$ (1/eV atom)
3.0000	3.406	110.1	0.652	0.2095
3.0198	3.514	110.5	0.660	0.2122
3.0341	3.662	110.5	0.672	0.2145
3.0503	3.864	110.4	0.688	0.2158
3.0639	4.020	110.1	0.704	0.2192
3.0758	4.175	109.4	0.718	0.2199
3.0784	4.210	109.3	0.722	0.2204
3.0874	4.340	109.0	0.735	0.2250
3.0994	4.550	107.9	0.756	0.2282
3.1080	4.712	107.7	0.773	0.2341
3.1191	4.925	106.0	0.796	0.2438
3.1283	5.104	105.6	0.817	0.2493

^aValues of T_c taken from a smooth curve through the data in Table I, data in Ref. 23, and those reported by G. Chanin, E. A. Lynton, and B. Serin, Phys. Rev. 114, 719 (1959).

it seems reasonable to expect a smaller effect of this kind in an alloy. In any case, it is clear that $N(E_F)$ increases much more rapidly with Z just above $Z = 3.09$ than just below.

The density of states at the Fermi surface can be calculated from γ . However, band-structure calculations give the "band density of states" $N_{bs}(E_F)$ which does not include the effects of phonon enhancement. These quantities are related by

$$(1 + \lambda)N_{bs} = N(E_F) = 3\gamma/2\pi^2 k_B^2, \quad (2)$$

where k_B is Boltzmann's constant. McMillan²⁶ has shown that λ is related to T_c and Θ_0 by

$$T_c = 1.45\Theta_0 \exp\left(-\frac{1.04(1 + \lambda)}{\lambda - u^*(1 + 0.62\lambda)}\right), \quad (3)$$

where u^* represents the Coulomb repulsion, and is in turn related to the isotope-shift coefficient α by

$$u^* = (1 - 2\alpha)^{1/2} \left(\frac{1 + 0.62\lambda}{1 + \lambda}\right)^{1/2} \left(\ln \frac{\Theta_0}{1.45T_c}\right). \quad (4)$$

Equation (3) was derived for a particular phonon spectrum, but it should be an adequate approximation in the present case since the relation between T_c and λ is not expected to be sensitive to details of the phonon spectrum for weak or intermediate coupling²⁶ ($\lambda < 1$). Following Morel and Anderson,³⁴ McMillan has suggested that $u^* \approx 0.1$ can be used in applying Eq. (3) to the simple (nontransition) polyvalent metals. This would correspond to $\alpha = 0.46$, whereas the experimental data³⁵ for the isotope effect in indium are represented by $\alpha = 0.50 \pm 0.03$. We have taken $u^* = 0.07$, which is the highest value that is reasonably consistent with the experimental data, in deriving the λ values given in Table III and in Fig. 6. The error in λ associated with the uncertainty u^* is not likely to be greater than that resulting from approximations in the derivation of Eq. (3), and the qualitative behavior of λ vs Z is independent of the value of u^* for $0 < u^* < 0.1$. The values of Θ_0 and T_c used in calculating λ were taken from smooth curves through the Θ_0 and T_c data.

The band density of states, calculated from Eq. (2), is also given in Table III and is plotted in Fig. 6. The change in slope of $N_{bs}(E_F)$ in the vicinity of $Z = 3.09$ is conspicuous, although it is smaller than the corresponding effect in γ —as expected from the Z dependence of T_c , which requires a change in the slope of λ vs Z . It seems reasonable to associate the change in slope of $N_{bs}(E_F)$ with the appearance of a new part of the Fermi surface as Z increases through the value of 3.09. In the hope that it will suggest a more detailed interpretation, we now turn to a consideration of the electronic

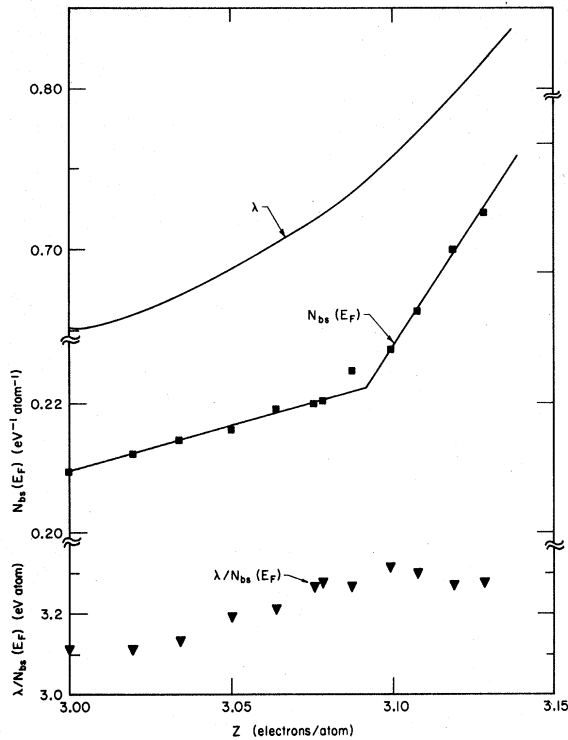


FIG. 6. The electron-phonon coupling constant, the band density of states, and their ratio, as a function of the conduction-electron/atom ratio.

structure of pure indium.

Figure 7(a) shows the first Brillouin zone for indium with certain symmetry points that are important to the following discussion labeled. The two types of inequivalent corners are represented by the point W with coordinates $(1, 0, \frac{1}{2}\alpha)$ and by the two points T with coordinates $(1 - \frac{1}{2}\alpha^2, 0, \alpha)$ and $(1, \frac{1}{2}\alpha^2, 0)$, where $\alpha = a/c$, the axial ratio of the reciprocal lattice. A free-electron Fermi sphere containing three electrons per atom falls just inside the corners W and just outside the corners T. The Fermi surface for (nearly) free electrons would therefore consist of pockets of holes in the first zone at the corners W; a second-zone surface multiply connected at W; third-zone tubes of electrons, called the β arms, around the edges of the square faces (perpendicular to $[001]$), and other tubes, called the α arms, connected to the β arms at T and extending part way toward W; and pockets of fourth-zone electrons at T. A possible Fermi surface for indium¹⁻⁶ is shown in Figs. 7(b) and 7(c). The pockets of holes in the first zone and of electrons in the fourth zone have been eliminated by the finite crystal potential; the α arms have been abbreviated and severed from the β arms; and the second-zone surface has been left multiply connected at the W corners. The two points of uncertainty are the existence of the α -arm remnants and the second-zone

connecting tubes. The α arms have been observed in some de Haas-van Alphen experiments,³ but not in others designed specifically to verify their existence,³⁶ and not in cyclotron resonance⁵ or radio-frequency size-effect⁶ measurements. The magnetic field dependence of the electrical resistivity gives no indication of the presence of open orbits, but it is difficult to assign an upper limit to the cross section of second-zone connecting tubes from these measurements.⁴ It has been suggested⁸ that some evidence for the second-zone connecting tubes may be found in the de Haas-van Alphen³ and radio-frequency size-effect measurements.⁶

Ashcroft and Lawrence⁸ have used the pseudopotential method to treat the band structure of indium. A model potential characterized by a single adjustable parameter R_c , which measures the range of pseudopotential cancellation in the core region, was used to fit the de Haas-van Alphen measurements³ of the extremal areas of the β arms. The experimental data for the β arms were fitted by two values of R_c , 0.575 and 0.715 Å. For $R_c = 0.575$ Å, there are small remnants of the α arms and the second-zone surface is multiply connected by small connecting tubes at W. For this model, an increase in the Fermi energy of 0.035 eV would replace the second-zone connecting tubes by pockets of third-zone electrons. For $R_c = 0.715$ Å, the α arms have completely disappeared and would contribute to the density of states only if the Fermi energy were in-

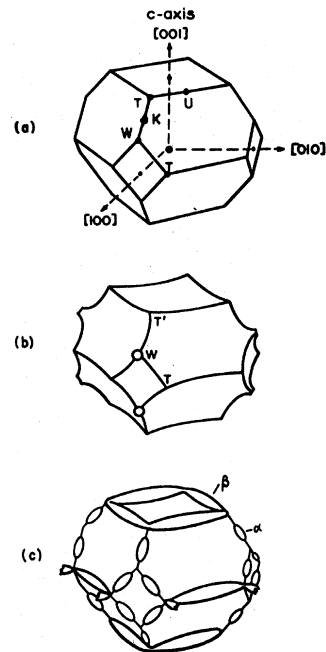


FIG. 7. (a) First Brillouin zone for indium. Certain points that are important to the discussion are labeled. (b) Possible second-zone Fermi surface for indium. (c) Possible third-zone Fermi surface for indium.

creased by about 0.4 eV. The lowest-energy fourth-zone states are over 1 eV higher than E_F for both models. Ashcroft and Lawrence cite a number of details of the Fermi-surface which are in better agreement with the 0.575-Å model than with the 0.715-Å model. The general shape of the density-of-states curve is also in better agreement with photoemission experiments³⁷ for $R_c = 0.575$ Å than for 0.715 Å.

The theoretically derived band structure suggests that the pieces of Fermi surface that might appear with increasing E_F , and therefore with increasing Z , are: (i) pockets of third-zone electrons at W when $\Delta E_F \approx 0.35$ eV for the $R_c = 0.575$ Å model; (ii) the α arms at K, when $\Delta E_F \approx 0.4$ eV for the $R_c = 0.715$ -Å model; and (iii) pockets of fourth-zone electrons at T when $\Delta E_F \approx 1.3$ eV for the $R_c = 0.575$ -Å model, or when $\Delta E_F \approx 1.5$ eV for the 0.715-Å model. The actual increase in E_F for a $Z = 3.09$ alloy over that for pure indium can be estimated from the "experimental" $N_{bs}(E_F)$. From $dE_F = N_A dZ / N_{bs}(E_F)$, where N_A is Avogadro's number, we obtain $\Delta E_F = 0.20$ eV. This estimate does not take into account the increase in volume with increasing tin content, but that is probably the best practical approximation for comparison with band-structure calculations which are based on constant volume. Two additional factors complicate the comparison of this estimate with band-structure calculations. First, it must be expected that the replacement of 9% of the indium atoms with tin atoms changes the crystal potential and the energy gaps. There seems to be no simple basis for estimating this effect, and we must recognize a consequent uncertainty in the energy gaps. Second, the c/a ratio increases with increasing Z , moving the points K and W further from the center of the zone and the β arms at U closer. For pure indium, it is clear that the Fermi surface contacts the boundary between the second and third zones along the edges containing the points K and near W, and that there is very little, if any, overlap. This configuration corresponds to a minimum in the energy of the occupied states in those regions. It seems probable that the increasing tetragonality of the lattice with increasing Z , which tends to favor this configuration and put the additional electrons into the β arms or the second zone, is associated with this contribution to the stability of the lattice. The trend to increased c/a ratio would stop, or be reversed, when the associated elastic strain finally forces substantial overlap into the third zone. The lattice-parameter data¹⁴ suggest that this might occur at $Z \approx 3.09$. Until this happens, however, it must be expected that the occupation of third-zone states at K or W will proceed more slowly with increasing Z than if the lattice were rigid. For this reason, the band-structure calculations can be expected to

underestimate the ΔE_F necessary to produce occupation of these states in the alloys.

From the theoretical energy gaps, it seems safe to conclude that occupation of fourth-zone states does not occur in these alloys and that the overlap which occurs at $Z = 3.09$ is into the third zone at either K or W. However, neither the band-structure calculations nor the experimental Fermi-surface studies suggest a clear choice between the latter possibilities. The possible errors in the theoretical energy gaps and the complications in comparing calculations for pure indium with experimental data on alloys prevent a choice based on a comparison of theoretical and experimental ΔE_F 's. If, in spite of the bulk of experimental evidence, it is assumed that the α arms are present in indium, the $R_c = 0.575$ -Å model is clearly more accurate. The occupation of third-zone states at W for that model when $\Delta E_F = 0.035$ eV would be a reasonable explanation of the increase in $dN_{bs}(E_F)/dZ$ at $Z = 3.09$. If it is assumed that the α arms are not present in indium, their appearance at $Z = 3.09$ could explain the $N_{bs}(E_F)$ data. In that case, neither model potential would provide a good fit to all experimental data, and the discrepancy between the theoretical and experimental ΔE_F 's would not be more serious than other failures of the model. A more detailed interpretation of the increase in $dN_{bs}(E_F)/dZ = 3.09$ – for example, a decision as to whether it is states at K or W that are occupied – requires, as a minimum, a resolution of the question of the presence of the α arms in indium. This might limit the possibilities for the change in the Fermi surface that occurs at $Z = 3.09$, and would also be helpful in choosing between various model potentials.

B. Electron-Phonon Coupling

For pure indium, a value for λ can also be derived by comparison of the experimental γ with the theoretical $N_{bs}(E_F)$. For the second-zone hole surface and the β arms alone, Ashcroft and Lawrence³ found $N_{bs}(E_F) = 0.24 \text{ eV}^{-1} \text{ atom}^{-1}$ and comparison with $\gamma = 1.633 \text{ mJ mole}^{-1} \text{ K}^{-2}$ using Eq. (2) gives $\lambda = 0.49$. The agreement with the value $\lambda = 0.65$ obtained from Eq. (3) is perhaps as good as can be expected in view of the approximations in the derivation of Eq. (3) and in the band-structure calculations. However, the effective masses for a number of second-zone and β -arm orbits obtained by comparing the results of cyclotron-resonance experiments with the theoretical band structure also suggest that the correct λ may be somewhat higher than 0.49.³⁸ This is perhaps an indication that the estimate of the total density of states is less accurate than the band structure. [Ashcroft and Lawrence obtained a higher λ value by comparing the calculated $N_{bs}(E_F)$ with an experimental γ value²⁹ that is almost certainly too high.] For a number of simple metals, Allen and

Cohen³⁹ have calculated λ directly from the phonon spectra and various pseudopotentials. For indium they found values between 0.84 and 1.16, depending on the pseudopotential.

The increase in λ with increasing Z for $3.00 < Z < 3.09$ is also consistent with the accommodation of the additional electrons in the β arms and the enhancements observed for β -arm orbits in cyclotron-resonance experiments. Comparison of cyclotron masses for β -arm orbits with the theoretical band structure gives consistently greater phonon enhancements for these orbits than for second-zone orbits.⁴⁰

The mean-square electron-phonon matrix element and $N_{bs}(E_F)$ both occur as factors in λ . It has been suggested that electron states close to strongly scattering Bragg planes, which are mixtures of several orthogonalized plane waves with large amplitudes, make larger contributions to the matrix-element factor than states that are more remote from Bragg planes.⁴¹ The variation of λ for $3.00 < Z < 3.09$ is consistent with this principle and the increasing contribution of β -arm states relative to that of second-zone states. As shown in Fig. 6, λ increases more rapidly than $N_{bs}(E_F)$ in this region. At $Z = 3.09$, however, where it seems clear that third-zone states, either near K or at W, begin to be occupied, the trend in $\lambda/N_{bs}(E_F)$ is reversed. This shows that the continued increase of λ for

$Z > 3.09$ can be accounted for entirely by the increase in area of the Fermi surface and, possibly, by large band masses associated with the new area. The apparent decrease in the contribution of the matrix-element factor seems to be in disagreement with the principle mentioned above.

V. CONCLUSION

An increase in $dN_{bs}(E_F)/dZ$ occurs in the neighborhood of $Z = 3.09$, where earlier measurements of T_c and lattice parameters had indicated a Brillouin-zone-boundary-Fermi-surface interaction. Comparison with theoretical and experimental band-structure studies on pure indium strongly suggests that the increase is associated with the occupation of new third-zone states, but it is not possible to specify precisely the location of these states. For $3.00 < Z < 3.09$, where additional electrons are accommodated in the second-zone and β -arm states, the increase in λ with increasing Z is a consequence of increases in both $N_{bs}(E_F)$ and the mean-square electron-phonon matrix element. For $Z > 3.09$, the continued increase in λ is apparently produced entirely by an increase in $N_{bs}(E_F)$. The variation of Θ_0 with Z is much smaller than that of T_c , and the trend in T_c is determined largely by that in λ .

[†]Work supported by the U. S. Atomic Energy Commission.

*Present address: Faculté des Sciences, Avenue F-D. Roosevelt, 50, Université Libre de Bruxelles, Bruxelles, Belgium.

†Present address: Department of Physics, University of the Witwatersrand, Jan Smuts Avenue, Johannesburg, South Africa.

¹J. A. Rayne and B. S. Chandrasekhar, Phys. Rev. **125**, 1952 (1962).

²J. A. Rayne, Phys. Rev. **129**, 652 (1963).

³G. B. Brandt and J. A. Rayne, Phys. Rev. **132**, 1512 (1963); Phys. Letters **12**, 87 (1964).

⁴Yu. P. Gaidukov, Zh. Eksperim. i Teor. Fiz. **49**, 1049 (1965) [Soviet Phys. JETP **22**, 730 (1966)].

⁵R. T. Mina and M. S. Khaiksin, Zh. Eksperim. i Teor. Fiz. **48**, 111 (1965) [Soviet Phys. JETP **21**, 75 (1965)].

⁶V. F. Gantmakher and I. P. Krylov, Zh. Eksperim. i Teor. Fiz. **49**, 1054 (1965) [Soviet Phys. JETP **22**, 734 (1966)].

⁷G. D. Gaspari and T. P. Das, Phys. Rev. **167**, 660 (1968).

⁸N. W. Ashcroft and W. E. Lawrence, Phys. Rev. **175**, 938 (1968).

⁹R. W. Shaw, Jr. and N. V. Smith, Phys. Rev. **178**, 985 (1969).

¹⁰W. Betteridge, Proc. Phys. Soc. (London) **50**, 519 (1938).

¹¹N. Ridley, J. Less-Common Metals **8**, 354 (1965).

¹²C. Tyzack and G. V. Raynor, Trans. Faraday Soc. **50**, 675 (1954).

¹³C. G. Fink, E. R. Jette, S. Katz, and F. J. Schnettler, Trans. Electrochem. Soc. **88**, 229 (1945).

¹⁴M. F. Merriam, Phys. Rev. Letters **11**, 321 (1963).

¹⁵M. F. Merriam, Rev. Mod. Phys. **36**, 152 (1964).

¹⁶M. F. Merriam, Phys. Rev. **144**, 300 (1966).

¹⁷N. Ridley, Phys. Letters **25A**, 134 (1967).

¹⁸C. M. Preece and H. W. King, Acta Met. **17**, 21 (1969).

¹⁹H. Jones, Proc. Roy. Soc. (London) **A147**, 396 (1934).

²⁰J. B. Goodenough, Phys. Rev. **89**, 282 (1953).

²¹K. Yonamitsu, J. Phys. Soc. Japan **21**, 1231 (1966).

²²I. V. Svechkarov, Zh. Eksperim. i Teor. Fiz. **47**, 960 (1964) [Soviet Phys. JETP **20**, 643 (1965)].

²³M. F. Merriam and M. VonHerzen, Phys. Rev. **131**, 637 (1963).

²⁴M. F. Merriam, Phys. Letters **17**, 16 (1965).

²⁵E. E. Havinga, in *Proceedings of the Eleventh International Conference on Low-Temperature Physics*, St. Andrews, 1968, edited by J. F. Allen, D. M. Finlayson, and D. M. McCall (University of St. Andrews Printing Department, St. Andrews, Scotland, 1969), Vol. II, p. 756.

²⁶W. L. McMillan, Phys. Rev. **167**, 331 (1968).

²⁷J. C. F. Brock, N. E. Phillips, and M. F. Merriam (unpublished).

²⁸H. R. O'Neal and N. E. Phillips, Phys. Rev. **137**, A748 (1965).

²⁹J. R. Clement and E. H. Quinnell, Phys. Rev. **92**, 258 (1953).

³⁰C. A. Bryant and P. H. Keesom, Phys. Rev. **123**, 491 (1961).

³¹H. W. White and D. C. McCollum, Phys. Rev. **B 1**,

552 (1970).

³²B. S. Chandrasekhar and J. A. Rayne, *Phys. Rev. Letters* **6**, 3 (1961).³³D. K. Finnemore and D. E. Mapother, *Phys. Rev.* **140**, 507 (1965).³⁴P. Morel and P. W. Anderson, *Phys. Rev.* **125**, 1263 (1962).³⁵N. M. Senozan, thesis, University of California, Berkeley, 1965 (unpublished). A preliminary report was given by H. R. O'Neal, N. M. Senozan, and N. E. Phillips, in *Proceedings of the Eighth International**Conference on Low-Temperature Physics, London*, 1962 (Butterworths, London, 1963), p. 403.³⁶A. J. Hughes and A. H. Lettington, *Phys. Letters* **27A**, 241 (1968).³⁷R. Koyama, W. E. Spicer, N. W. Ashcroft, and W. E. Lawrence, *Phys. Rev. Letters* **19**, 1284 (1967).³⁸See Fig. 13 and Table III of Ref. 8.³⁹Philip B. Allen and Marvin L. Cohen, *Phys. Rev.* **187**, 525 (1969).⁴⁰See Table III of Ref. 8.⁴¹E. E. Havinga, *Phys. Letters* **26A**, 244 (1968).

PHYSICAL REVIEW B

VOLUME 3, NUMBER 6

15 MARCH 1971

Electrical Transport Properties of Thin Bismuth Films*

R. A. Hoffman[†] and D. R. Frankl*Department of Physics, The Pennsylvania State University, University Park, Pennsylvania 16802*

(Received 25 August 1970)

The resistivity, Hall coefficient, and magnetoresistance coefficient of well ordered but twinned bismuth films were measured between 1.15 and 300 K. It was found that the surface scattering in these films is not specular, contrary to the findings of some other workers. At 300 K the thickness dependence of the resistivity can be roughly fitted by the Fuchs-Sondheimer boundary-scattering theory with a surface reflection coefficient of 0.6, indicating partially diffuse scattering. It was also observed that the apparent surface scattering becomes more diffuse with decreasing temperature until at low temperatures the data can no longer be explained by the Fuchs-Sondheimer theory. This indicates that an additional size-dependent temperature-dependent scattering mechanism exists in thin-film transport. It was observed that at low temperatures the temperature dependence of the conductivity could be explained on the basis of a constant mean free path for the thicker samples. For thinner samples, the temperature dependence of the conductivity again indicates that there is an additional scattering mechanism that becomes stronger with decreasing temperature and decreasing sample thickness. Values of the mobility and mean free path, calculated from the data, were also observed to vary consistently with the sample thickness. The conclusions, drawn from the thickness dependence of the resistivity, concerning the diffuseness of the surface scattering of the charge carriers were confirmed by the dependence of the mean free path upon the sample thickness. Finally, quantum size-effect oscillations were observed in all of the transport properties of the thin bismuth films at low temperatures. The period (about 400 Å) and phase of the oscillations are in reasonable agreement with the theory and in good agreement with other values reported in the literature.

I. INTRODUCTION

There are two types of size effects observable in thin metal samples. The "ordinary size effect," which is seen when the charge-carrier mean free path is comparable with or greater than the sample thickness, results in a resistivity which is higher than the bulk value, due to the additional scattering of the charge carriers at the sample surface. The "quantum size effect," which manifests itself when the carrier wavelength is comparable with or greater than the sample thickness, consists of oscillations in the transport properties as a function of the sample thickness with a period approximately equal to one-half of the carrier wavelength.

An approximate expression for the ordinary size effect in thin films was derived by Thomson¹ in

1901, and a more rigorous expression was obtained by Fuchs² in 1938. In 1952 Sondheimer³ wrote a review article on the size effect in which he expanded and improved some of the earlier calculations. The Fuchs-Sondheimer theory contains two independent parameters: k , which is the ratio of the sample thickness to the bulk-carrier mean free path, and P , the surface reflection coefficient. P is defined as the fraction of the carriers that are reflected specularly at the surface of the sample. At the time of Sondheimer's article there appeared to be good agreement between experiments on thin metal foils⁴ and the theory with $P = 0$, indicating completely diffuse surface scattering.

One feature of the theory is that for perfectly specular scattering ($P = 1$) there is no size effect, and for $P < 1$ the conductivity tends toward zero as